Article

A Subwavelength Transmit-Array Lens Element Combining Functions of Phase Modulation and Polarization Conversion

T. Xu [1], Y. Lu [1], G. He [2,*] and X. Yang [2,*]

[1] School of Communication and Information Engineering, Shanghai University, Shanghai 200444, China; xutao85c56@163.com (T.X.); lyyumy123@163.com (Y.L.)

[2] Shanghai Institute for Advanced Communication and Data Science, Key Laboratory of Specialty Fiber Optics and Optical Access Networks, Shanghai University, Shanghai 200444, China

[*] Correspondence: ghe@shu.edu.cn (G.H.); yang.xx@shu.edu.cn (X.Y.)

Abstract: Advanced applications require transmit-array lenses featuring low profiles, covering 360° phase modulation, and, potentially, polarization conversion. Subwavelength metamaterial elements with multilayers manipulate electromagnetic waves with predesigned phase shifts, resulting in the transmit-array lens's low profile and light weight. Conventional designs separate the transmit-array lens and polarization converter with two functional devices and suffer from high profiles and complicated mechanical assembly. In order to resolve these issues, a subwavelength lens element combining the functions of phase modulation and polarization conversion is proposed. The metamaterial lens element consists of phase modulation, linear-circular polarization conversion modules, and a metallic via structure electrically connecting these two modules. The multifunctional lens element modulates the transmitted phase with a three-bit phase shift and operates in the frequency range from 24.5 to 27 GHz, with less than −10 dB reflection coefficient, 1 dB transmission loss, and a 2.5 dB axial ratio. A transmit-array lens antenna with the proposed element is implemented to validate the abilities of beam focus and polarization conversion. The gain of the lens antenna reaches 26.3 dBi, with a 3 dB beamwidth of 6.7° and −18 dB sidelobe level, and the axial ratio of the converted circular polarization is below 1 dB. The aperture efficiency of the antenna is 45.2%.

Keywords: transmit array; lens; phase modulation; polarization conversion

1. Introduction

Modern wireless communication systems, such as 5G, satellite communications, and wireless access, require an antenna possessing multiple features, such as high directivity, low sidelobe level (SLL), high efficiency, and multiple polarization operation. Transmit-array lens antennas show high flexibility in the manipulation of radiating electromagnetic waves by utilizing subwavelength metal-dielectric elements [1–10], which satisfies the requirements of the wireless communication systems for these special applications, thus raising increased research interest in both academic and industrial domains.

Fixed-beam, high-performance transmit arrays operating in single-linear and dual-polarization modes have been thoroughly demonstrated [1–15]. A wideband linearly polarized transmit-array antenna with a high gain of 33.45 dBi and high efficiency of 44.03% is proposed at 150 GHz for fixed beam applications [1]. A dual-band transmit-array antenna with low scan loss is designed with operating frequencies 19.5 GHz and 29 GHz, which achieves scanning performance of ±40° and ±30°, independently, with 2 dB scan loss [7]. A 4 × 4 scanning-phased array antenna with leaky-wave, enhanced lenses operating at 28 GHz is proposed [8]. It is designed with dual polarization and achieves a 20% relative bandwidth and a gain of 26.2 dBi. A circularly polarized transmit-array lens antenna is proposed in [9], which realizes beam steering at Ka-band by in-plane translation of a plate lens antenna. It achieves a gain of 27.3 dBi and a scanning angle of 0° to 50° with a 2.8 dB scan loss. A transmit-array antenna with linear-to-circular polarization at Ka-band is

implemented with a high gain of 33.8 dBi, 1 dB bandwidth of 9.2%, and aperture efficiency of 51.2% [10]. The transmit-array antenna utilizes a half-wavelength unit-cell element and modulates the transmitted wave phase by rotating the element.

In order to realize the polarization conversion function, a separate metamaterial polarization converter is commonly implemented. A fixed-beam transmit-array and metamaterial polarization converter are combined to realize the high gain and linear-to-circular polarization conversion. Several metamaterial polarization converters have been investigated for linear-to-circular polarization conversion [16–25]. A cross-polarization converter uses metalized vias to convert linearly polarized incident electromagnetic wave into its orthogonal-corresponding electromagnetic wave [16]. Its conversion efficiency is 98.6% at 8.79 GHz when the incident angle is normal. A dual-band dual-linear-to-circular polarization converter can convert x-polarization to left-handed circular polarization at a lower band and right-handed circular polarization at a higher band [17]. A polarization converter to convert a linearly polarized incident wave into an outgoing circularly polarized wave is proposed in [18], which is constructed by a two-dimensional array of thin cavities with etched slots. The polarization converter features an extremely low insertion loss of around 0.1 dB and a high polarization conversion efficiency of 0.97. A wideband polarization converter is designed in [19], where a multilayer frequency-selective surface structure is employed to achieve a broad operating frequency range. By rotating the proposed polarization converter, the incident wave can transform in four cases: left- and right-handed circular polarization waves and horizontal and vertical polarization waves.

In this paper, we proposed a transmit-array lens element that can realize both phase modulation and polarization conversion functions at the same time. The lens element consists of phase modulation, linear-circular polarization conversion modules, and a metallic via structure connecting these two modules. When the lens unit works at 24.5–27 GHz, it can convert linear polarization wave into circular polarization wave with phase coverage of 360°, reflection coefficient lower than −10 dB, transmission loss of 1 dB, and an axial ratio of 2.5 dB.

The paper is organized as follows: The design of the transmit-array lens element and simulated results are presented in Section 2. In Section 3, a transmit-array structure with the proposed lens element is proposed and its performance is simulated. Finally, the paper is concluded in Section 4.

2. Transmit-Array Element Structure

A transmit-array lens element that can realize phase modulation and polarization conversion functions at the same time is shown in Figure 1. The element consists of six layers of metal patterns, five layers of dielectric substrates, and a metalized via. The first four-layer metallic patterns with substrates form a phase modulation part, as shown in Figure 1a. The split ring resonator with substrate functions as a linear-to-circular polarization conversion part. The fifth layer is a metal ground with circular holes to isolate these two parts as shown in Figure 1b, and the phase modulation and polarization conversion parts are electrically connected through a metallic via. All layers of the metal patterns are printed on dielectric substrates of Rogers RT5880 with εr = 2.2, $\tan\delta$ = 0.0009, and M1 = 0.75 mm. The period of the element is S = 3.6 mm. In the electromagnetic simulation software HFSS, we optimized the geometric dimensions of nine elements under periodic boundary conditions and Floquet port excitations. In the frequency range of 24.5–27 GHz, the element provides a phase shift of 40°, covers 360° with three-bit phase modulation, and demonstrates horizontally linear polarization to right-hand circular polarization. The geometric dimensions of all unit-cells are shown in Table 1. The phase shift varies with the size parameters of the unit cell. Among them, the radius of the metalized via R_via and the outer radius of the metallic open ring R_out are sensitive to the axial ratio, transmitted amplitude, and phase modulation of the unit cells. According to the state-of-the-art fabrication processing, the minimum fabrication size is 25 μm for the multilayer PCB. The variations in transmission coefficient with R_via and R_out are shown in Figure 2. When R_via and R_out change

± 25 μm, the axial ratio, transmission coefficient, and phase of the unit cell change about ± 0.4 dB, ± 0.5 dB, and $\pm 5°$ over the frequency range of 24.5–27 GHz, respectively, which is tolerated for the transmit-array phase distribution.

(a)

(b)   (c)
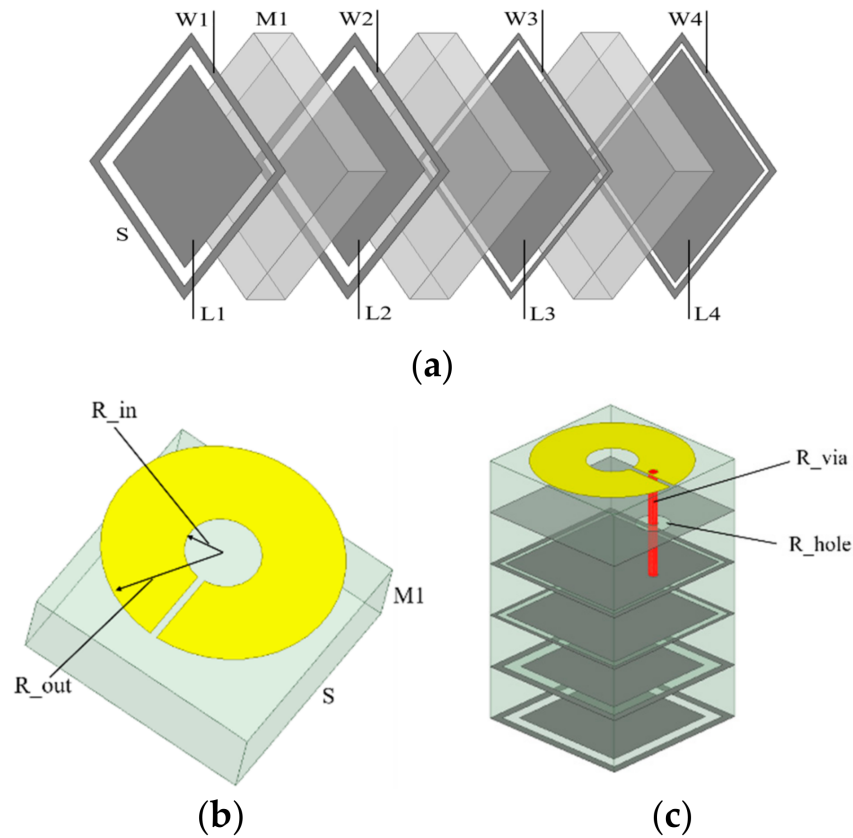
Figure 1. Schematic diagram of the proposed lens element: (**a**) phase modulation part; (**b**) polarization modulation part; (**c**) 3D view.

Table 1. Geometric parameters of the nine unit cells.

	L1	L2	L3	L4	W1	W2	W3	W4	R_in	R_out
Unit-cell1	2.58	2.34	2.3	2.92	0.1	0.18	0.1	0.13	0.4	1.69
Unit-cell2	2.85	2.71	2.67	2.89	0.18	0.18	0.1	0.13	0.39	1.7
Unit-cell3	2.56	2.7	3.11	3.09	0.18	0.19	0.14	0.12	0.39	1.69
Unit-cell4	2.14	1.98	1.62	2.68	0.19	0.25	0.15	0.18	0.39	1.7
Unit-cell5	3.12	3.16	3.08	3.1	0.13	0.11	0.08	0.14	0.39	1.71
Unit-cell6	3.22	3.18	3.16	3.13	0.12	0.11	0.1	0.14	0.39	1.705
Unit-cell7	2.18	2.11	1.5	2.25	0.35	0.1	0.15	0.1	0.4	1.7
Unit-cell8	2.7	2.7	3.13	3.15	0.1	0.18	0.09	0.13	0.55	1.7
Unit-cell9	2.33	2.2	1.1	2.9	0.17	0.25	0.15	0.18	0.39	1.7
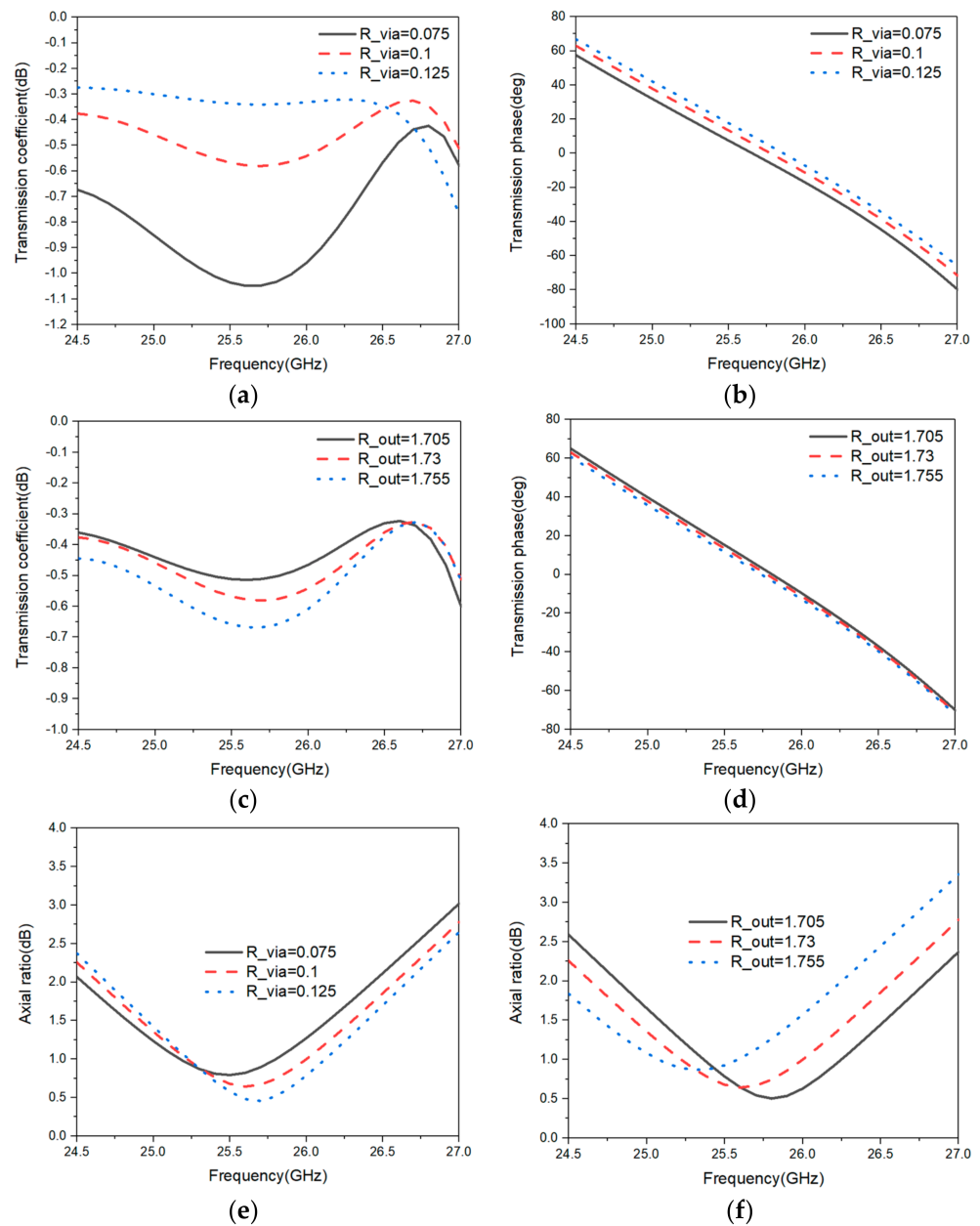
Figure 2. The influence of variations in R_via and R_out on the transmission coefficient, transmission phase, and axial ratio of the lens element over the frequency range of 24.5–27 GHz: (**a**) transmission coefficient of R_via in dB; (**b**) transmission phase of R_via in degrees; (**c**) transmission coefficient of R_out in dB; (**d**) transmission phase of R_out in degrees; (**e**) axial ratio of R_via in dB; (**f**) axial ratio of R_out in dB.

The simulated reflection coefficients, transmission phase, and axial ratio responses of the proposed transmit-array element versus the frequency are shown in Figure 3. The reflection coefficients of all lens unit cells are lower than −10 dB, the transmission phase of the lens unit-cells shifts with a step of 40° and covers 360°, and the axial ratio of all unit cells is less than 3 dB for the whole frequency range, from 24.5 GHz to 27 GHz. With the incident angle varying from 0° to 30°, the change in the transmission phase shift is less than nine degrees, as shown in Figure 3e. The element has no air layer and is easy to fabricate with PCB manufacturing. In order to highlight the advantages of this research, Table 2 lists comparative features of several elements in the published literature, including the center frequency, period of the element, thickness of the element, phase modulation, and polariza-

tion conversion. It can be seen from the table that only the elements in [10,24,25] and our proposed element support both phase modulation and polarization conversion in one unit. However, the element of the proposed element is a subwavelength structure, compared with the elements with half-wavelength size in [10,24,25], which means more units can be deployed in the same transmit-array aperture, with higher phase modulation diversity.
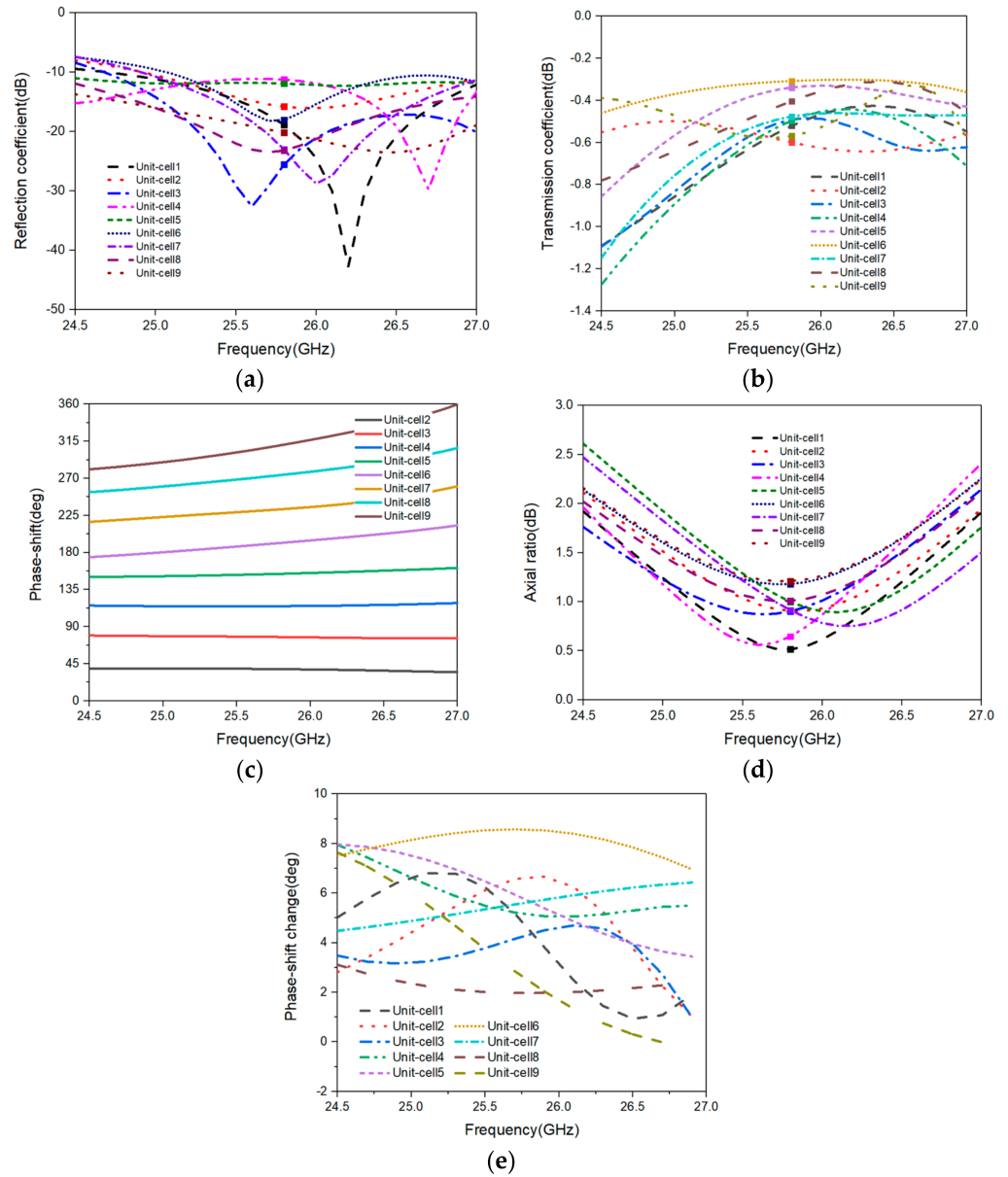
Figure 3. Phase modulation and polarization conversion properties of the proposed lens element over the frequency range 24.5–27 GHz: (**a**) reflection coefficient in dB; (**b**) transmission coefficient in dB; (**c**) phase shift in degrees; (**d**) axial ratio of the converted right-hand circular polarization in dB; (**e**) phase change for the incident wave varying from 0 degrees to 30 degrees.

Table 2. Comparisons of the elements.

Ref.	Center Frequency (GHz)	Period of the Element (λ_0)	Thickness of the Element (λ_0)	Phase Modulation	Polarization Transformation	Measurement
[1]	140	0.58	0.28	2 bit	×	√
[3]	12.25	0.6	0.5	3 bit	×	√
[9]	29.75	0.25	0.33	6 bit	×	√
[10]	29.5	0.5	0	3 bit	√	√
[11]	25	0.29	0.81	3 bit	×	√
[16]	9	0.48	0.06	×	√	√
[17]	25	0.44	0.09	×	√	√
[18]	10	0.72	0.11	×	√	√
[19]	9.4	0.31	0.19	×	√	√
[24]	27	0.54	0.18	2 bit	√	√
[25]	300	0.5	0.26	3 bit	√	√
This work	**25.8**	**0.31**	**0.32**	**3 bit**	√	×

3. Array Verification Lens Element Function

In order to verify the proposed functional unit-cell performance, a fixed-beam transmit-array with a $4\lambda_0 \times 4\lambda_0$ (λ_0 is the wavelength at the center operating frequency 25.8 GHz) size was designed and simulated. The schematic diagram of the transmit-array is shown in Figure 4a, and the phase distribution is demonstrated in Figure 4b. The transmit-array was fed with a horn antenna with a gain of 14.3 dBi and a focal length of 108 mm. The proposed transmit-array was studied using Ansys HFSS 2020. The gain pattern and axial ratio of several frequency points of the transmit-array in the frequency range of 24.5–27 GHz are presented in Figure 5. At 25.8 GHz, the gain of the main lobe with a 3 dB beamwidth of 6.7° reached 26.3 dBi, and the maximum SLL was −18 dB. Figure 6 presents the simulated co-polarization and cross-polarization gains versus frequency. The transmit array exhibited 11.5% 1 dB gain bandwidth. The maximum gain is 26.5 dBi, leading to the corresponding aperture efficiency of 45.2% at 25.8 GHz. Due to the existence of metallic vias and six metal-pattern layers in the transmit-array element, the fabrication processing became complicated and difficult, so we mainly focused on the design and novelty concept.

(a)

(b)
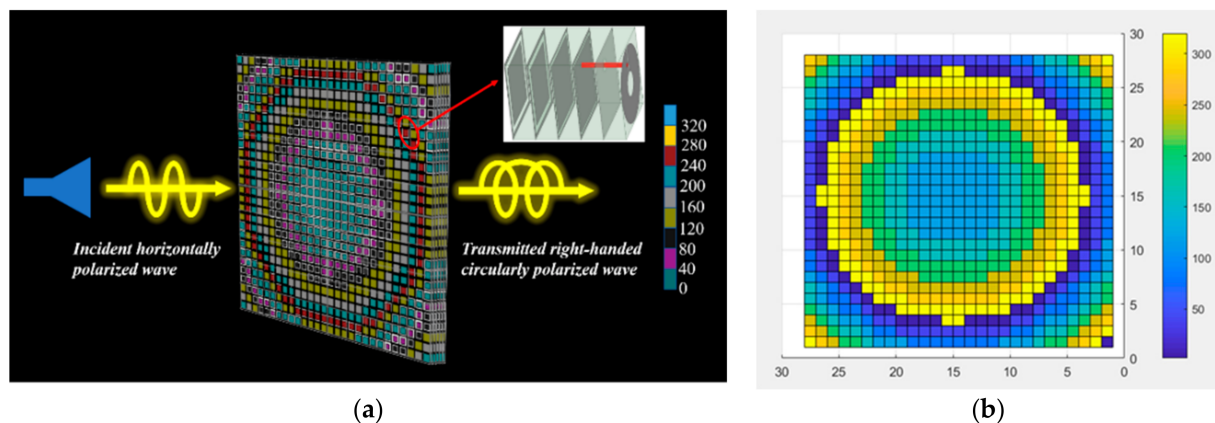
Figure 4. The designed transmit-array lens antenna with proposed elements: (**a**) schematic diagram of the transmit-array lens antenna; (**b**) phase distribution of the transmit-array antenna in degrees.
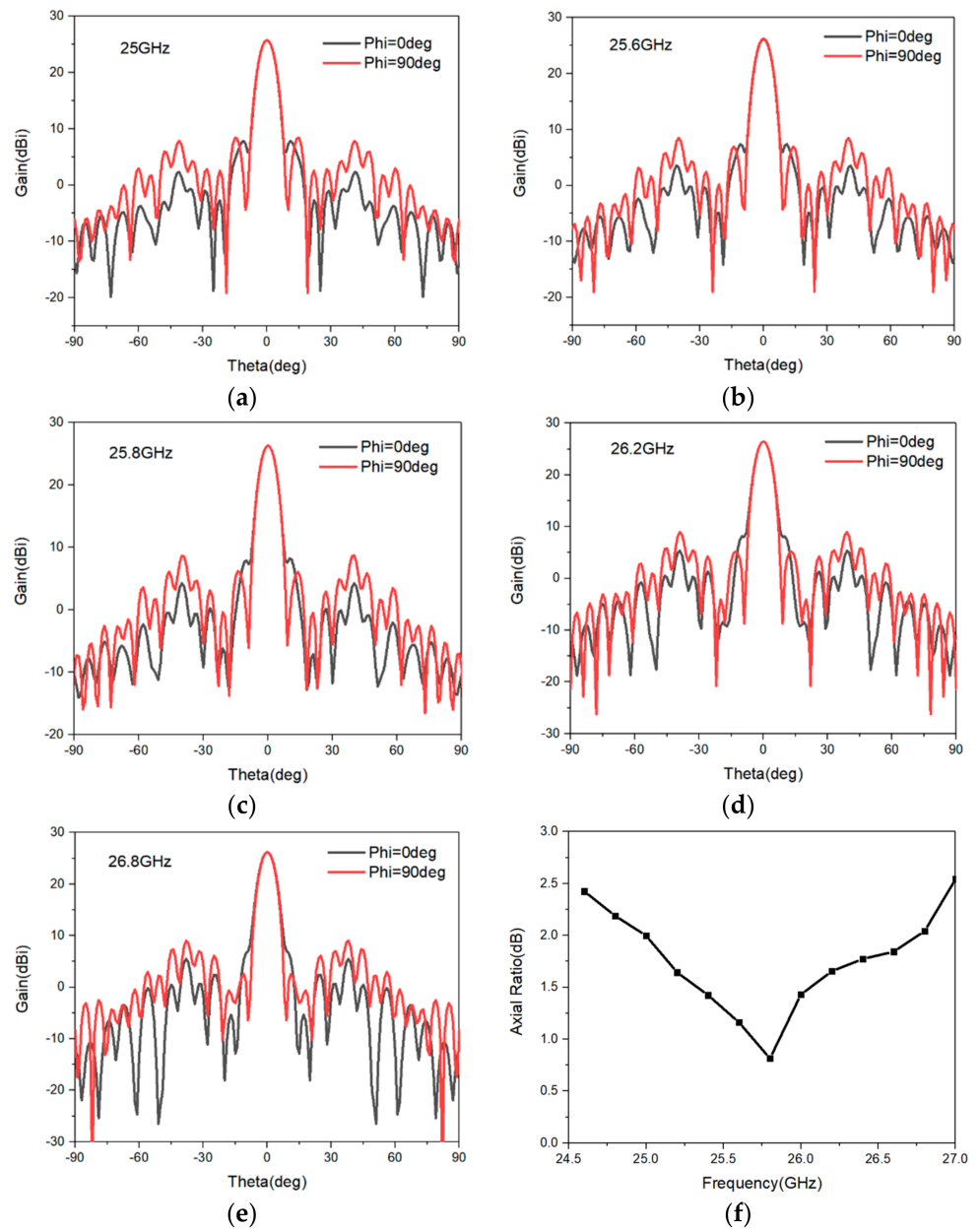
Figure 5. Radiation properties of the transmit-array with the proposed unit-cells over the frequency range 24.5–27 GHz: (**a**) gain pattern at 25 GHz; (**b**) gain pattern at 25.6 GHz; (**c**) gain pattern at 25.8 GHz; (**d**) gain pattern at 26.2 GHz; (**e**) gain pattern at 26.8 GHz; (**f**) axial ratio of transmit array in dB.
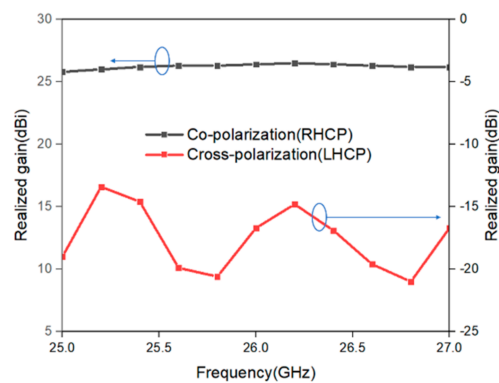
Figure 6. Co-polarization and cross-polarization gains of the transmit array versus frequency.

4. Conclusions

Numerical simulations confirmed that the proposed subwavelength transmit-array lens elements exhibited both phase modulation and polarization conversion functions with one unit. The phase-shift change in the transmit-array unit was less than 10°, with an incident angle varying 30°, which is tolerable for beam scanning of the transmit-array antenna. The lens element covers the frequency range of 24.5–27 GHz, modulates the transmitted wave with a three-bit phase shift covering 360°, and converts the linearly polarized incident wave into a circularly polarized wave. The reflection coefficients of the unit cells were lower than −10 dB, the transmission loss was lower than 1 dB, and the axial ratio was below 2.5 dB. In order to further verify the functions of the transmit-array lens element, the unit cells were arranged in a grid pattern to form a fixed-beam, transmit-array antenna. The simulated results showed that the gain of the transmit-array increased by 12 dB, and the axial ratio was lower than 1 dB. The proposed transmit-array lens element can be implemented into flexible transmit-array antennas for wireless communication applications.

Author Contributions: Supervision, G.H. and X.Y.; Validation, Y.L.; Writing—original draft, T.X. All authors have read and agreed to the published version of the manuscript.

Institutional Review Board Statement: Not applicable.

Informed Consent Statement: Not applicable.

Conflicts of Interest: The authors declare no conflict of interest.

References

1. Miao, Z.W.; Hao, C.H.; Luo, G.Q.; Gao, L. 140 GHz High-Gain LTCC-Integrated Transmit-Array Antenna Using a Wideband SIW Aperture-Coupling Phase Delay Structure. *IEEE Trans. Antennas Propag.* **2018**, *66*, 182–190. [CrossRef]
2. Jazi, M.N.; Chaharmir, M.R.; Shaker, J.; Sebak, A.R. Broadband transmitarray antenna design using polarization-insensitive frequency selective surfaces. *IEEE Trans. Antennas Propag.* **2016**, *64*, 99–108. [CrossRef]
3. Abdelrahman, A.H.; Elsherbeni, A.Z.; Yang, F. High-gain and broadband transmitarray antenna using triple-layer spiral dipole elements. *IEEE Antennas Wireless Propag. Lett.* **2014**, *13*, 1288–1291. [CrossRef]
4. Rahmati, B.; Hassani, H.R. High-effificient wideband slot transmitarray antenna. *IEEE Trans. Antennas Propag.* **2015**, *63*, 5149–5155. [CrossRef]
5. Erfani, E.; Niroo-Jazi, M.; Tatu, S. A high-gain broadband gradient refractive index metasurface lens antenna. *IEEE Trans. Antennas Propag.* **2016**, *64*, 1968–1973. [CrossRef]
6. Wu, R.Y.; Li, Y.B.; Wu, W.; Shi, C.B.; Cui, T.J. High-gain dual-band transmitarray. *IEEE Trans. Antennas Propag.* **2017**, *65*, 3481–3488. [CrossRef]
7. Pham, T.K.; Guang, L.; González-Ovejero, D.; Sauleau, R. Dual-Band Transmitarray With Low Scan Loss for Satcom Applications. *IEEE Trans. Antennas Propag.* **2021**, *69*, 1775–1780. [CrossRef]
8. Zhang, H.; Bosma, S.; Neto, A.; Llombart, N. A Dual-Polarized 27 dBi Scanning Lens Phased Array Antenna for 5G Point-to-Point Communications. *IEEE Trans. Antennas Propag.* **2021**, *69*, 5640–5652. [CrossRef]
9. Lima, E.B.; Matos, S.A.; Costa, J.R.; Fernandes, C.A.; Fonseca, N.J.G. Circular polarization wide-angle beam steering at Ka-band by in-plane translation of a plate lens antenna. *IEEE Trans. Antennas Propag.* **2015**, *63*, 5443–5455. [CrossRef]
10. Diaby, F.; Clemente, A.; Pham, K.T.; Sauleau, R.; Dussopt, L. Circularly Polarized Transmitarray Antennas at Ka-Band. *IEEE Antennas Wirel. Propag. Lett.* **2018**, *17*, 1204–1208. [CrossRef]
11. Matos, S.A.; Lima, E.B.; Silva, J.S.; Costa, J.R.; Fernandes, C.A. High gain dual-band beam-steering transmit array for satcom terminals at ka-band. *IEEE Trans. Antennas Propag.* **2017**, *65*, 3528–3539. [CrossRef]
12. Di Palma, L.; Clemente, A.; Dussopt, L.; Sauleau, R.; Potier, P.; Pouliguen, P. Circularly-polarized reconfigurable transmitarray in Ka-band with beam scanning and polarization switching capabilities. *IEEE Trans. Antennas Propag.* **2017**, *65*, 529–540. [CrossRef]
13. Matos, S.A.; Lima, E.B.; Costa, J.R.; Fernandes, C.A.; Fonseca, N.J.G. Design of a 40 dBi planar bifocal lens for mechanical beam steering at ka-band. In Proceedings of the 2016 10th European Conference on Antennas and Propagation (EuCAP), Davos, Switzerland, 10–15 April 2016.
14. Mao, C.; Gao, S.; Wang, Y. Broadband high-gain beam-scanning antenna array for millimeter-wave applications. *IEEE Trans. Antennas Propag.* **2017**, *65*, 4864–4868. [CrossRef]

15. Mumcu, G.; Kacar, M.; Mendoza, J. Mm-wave beam steering antenna with reduced hardware complexity using lens antenna subarrays. *IEEE Trans. Antennas Propag.* **2018**, *17*, 1603–1607. [CrossRef]

16. Xu, P.; Jiang, W.X.; Wang, S.Y.; Cui, T.J. An Ultrathin Cross-Polarization Converter With Near Unity Efficiency for Transmitted Waves. *IEEE Trans. Antennas Propag.* **2018**, *66*, 4370–4373. [CrossRef]

17. Naseri, P.; Matos, S.A.; Costa, J.R.; Fernandes, C.A.; Fonseca, N.J.G. Dual-Band Dual-Linear-to-Circular Polarization Converter in Transmission Mode Application to K/Ka-Band Satellite Communications. *IEEE Trans. Antennas Propag.* **2018**, *66*, 7128–7137. [CrossRef]

18. Wang, J.; Wu, W. Cavity-based linear-to-circular polarization converter. *Opt. Express* **2017**, *25*, 3805. [CrossRef]

19. Li, L.; Li, Y.; Wu, Z.; Huo, F.; Zhang, Y.; Zhao, C. Novel Polarization-Reconfigurable Converter Based on Multilayer Frequency-Selective Surfaces. *Proc. IEEE* **2015**, *103*, 1057–1070. [CrossRef]

20. Lin, B.; Wu, J.L.; Da, X.Y.; Li, W.; Ma, J.J. A linear-to-circular polarization converter based on a second-order band-pass frequency selective surface. *Appl. Phys. A Solids Surf.* **2017**, *123*, 43. [CrossRef]

21. Xu, P.; Wang, S.-Y.; Geyi, W. A linear polarization converter with near unity effifiency in microwave regime. *J. Appl. Phys.* **2017**, *121*, 144502. [CrossRef]

22. Abadi, S.M.A.M.H.; Behdad, N. Wideband linear-to-circular polarization converters based on miniaturized-element frequency selective surfaces. *IEEE Trans. Antennas Propag.* **2016**, *64*, 525–534. [CrossRef]

23. Sohail, I.; Ranga, Y.; Esselle, K.P.; Hay, S.G. A linear to circular polarization converter based on Jerusalem-cross frequency selective surface. In Proceedings of the 2013 7th European Conference on Antennas and Propagation (EuCAP), Gothenburg, Sweden, 8–12 April 2013; pp. 2141–2143.

24. Cao, Y.; Yang, W.; Xue, Q.; Che, W. A Broadband Low-Profile Transmitarray Antenna by Using Differentially Driven Transmission Polarizer With True-Time Delay. *IEEE Trans. Antennas Propag.* **2022**, *70*, 1529–1534. [CrossRef]

25. Koutsos, O.; Manzillo, F.F.; Clemente, A.; Sauleau, R. Design of a 3-Bit Transmitarray Antenna at 300 GHz using Asymmetric Linear Polarizers. In Proceedings of the 2020 IEEE International Symposium on Antennas and Propagation and North American Radio Science Meeting, Montreal, QC, Canada, 5–10 July 2020; pp. 1505–1506.